Climate Risk Management 47 (2025) 100686

Contents lists available at ScienceDirect

Climate Risk Management

journal homepage: www.elsevier.com/locate/crm

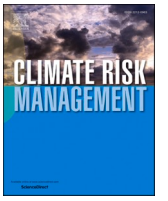

How beneficial are seasonal climate forecasts for climate risk management? An appraisal for crop production in Tanzania

Jacob Emanuel Joseph [a,c,*], K.P.C Rao [b], Elirehema Swai [d], Anthony M. Whitbread [c], Reimund P. Rötter [a,e]

[a] University of Göttingen, Tropical Plant Production and Agrosystems Modelling (TROPAGS), Grisebachstrasse 6, 37077, Göttingen, Germany
[b] International Crops Research Institute for the Semi-Arid Tropics (ICRISAT), Hyderabad, India
[c] International Livestock Research Institute (ILRI), Dar es Salaam, Tanzania
[d] Tanzania Agricultural Research Institute (TARI)- Makutupora, Dodoma, Tanzania
[e] University of Göttingen, Center of Biodiversity and Sustainable Land Use (CBL), Buesgenweg 1, 37077, Göttingen, Germany

ARTICLE INFO

Keywords:
APSIM
Climate risk management
Growing period
Onset dates
Seasonal climate forecasts
Sea surface temperature

ABSTRACT

Understanding growing period conditions is crucial for effective climate risk management strategies. Seasonal climate forecasts (SCF) are key in predicting these conditions and guiding risk management in agriculture. However, low SCF adoption rates among smallholder farmers are due to factors like uncertainty and lack of understanding. In this study, we evaluated the benefits of SCF in predicting growing season conditions, and crop performance, and developing climate risk management strategies in Kongwa district, Tanzania. We used sea surface temperature anomalies (SSTa) from the Indian and Pacific Ocean regions to predict seasonal rainfall onset dates using the k-nearest neighbor model. Contrary to traditional approaches, the study established the use of rainfall onset dates as the criterion for predicting and describing growing period conditions. We then evaluated forecast skills and the profitability of using SCF in crop management with the Agricultural Production System sIMulator (APSIM) coupled with a simple bio-economic model. Our findings show that SSTa significantly influences rainfall variability and accurately predicts rainfall onset dates. Onset dates proved more effective than traditional methods in depicting key growing period characteristics, including rainfall variability and distribution. Including SCF in climate risk management proved beneficial for maize and sorghum production both agronomically and economically. Not using SCF posed a higher risk to crop production, with an 80% probability of yield losses, especially in late-onset seasons. We conclude that while SCF has potential benefits, improvements are needed in its generation and dissemination. Enhancing the network of extension agents could facilitate better understanding and adoption by smallholder farmers.

1. Introduction

1.1. Background

In the tropics and sub-tropics, the growing period is meteorologically defined as the start and end of the rainy season i.e., the period

* Corresponding author.

https://doi.org/10.1016/j.crm.2024.100686
Received 5 November 2023; Received in revised form 18 December 2024; Accepted 31 December 2024
Available online 4 January 2025

in which crop growth and development are possible (Jätzold & Kutsch, 1982). However, a more pragmatic definition of the growing period includes the actual dates on which the farmers sow and harvest their crops (Shah et al., 2021). In rainfed systems, the intra-seasonal rainfall and temperature variations often lead to soil moisture fluctuations and significantly influence on-farm key operations such as sowing, thinning, weeding, and fertilizer applications. Crop productivity is highly reliant on effective timing and the influence of the growing period's characteristics in reducing the uncertainties of timing the key on-farm operations (Inthavong et al., 2011). For instance, the false onset of the rainy season may lead to early sowing, which negatively impacts crop growth due to water stress associated with prolonged dry spells after the first rain event.

An in-depth understanding of the growing period characteristics, including the amount and pattern of soil moisture availability, is important for both planning and conducting agricultural activities in a way that will enhance the productivity and sustainability of the production systems. For instance, Araya et al., 2010 showed how understanding the growing period characteristics, i.e., onset and length of the growing period, can be important in mitigating and adapting to potential impacts of climate variability and change. Their study applied the concept of growing period characterization using temperature, rainfall, and evapotranspiration to determine the onset and cessation of rainfall and the length of the growing period to find out more suitable teff (*Eragrostis tef*) and barley (*Hordeum vulgare*) growing zonesin Ethiopia.For instance, quick-maturing and drought-resistant varieties of teff and barley are recommended for central and eastern areas, while medium-maturing cultivars are suggested for the southwest. Their study highlighted useful climate risk management strategies for farmers and agronomists to better adapt and mitigate the impact of climate variability and change.

Seasonal climate forecasts (SCF)— prediction of the weather conditions over the next three to six months, including the amount of rain and temperature—have been used in various ways in climate risk management studies. For example, SCF has been used as a tool to guide farmers in various on-farm operations, such as providing information on the right time to sow and harvest their crops (Ceglar & Toreti, 2021; Diouf et al., 2020). The low rate of adoption of this useful information, especially among smallholder farmers in Africa, has been linked to a variety of factors, including the uncertainty and comprehensibility of the information presented (Ebhuoma, 2022; Guido et al., 2020). Traditionally, seasonal forecasts quantify the probability of the amount of rainfall in the coming season being below average, average, or above average. Although this kind of information might be useful in some aspects of planning ahead of the season, it explicitly excludes the distribution of the rainfall amounts, focusing instead on events that might greatly impact crop growth and productivity, such as dry and wet spells (Ebhuoma, 2022). The uncertainty of such forecasts increases with the increasing frequency of extreme events (Pohl et al., 2017), a consequence of global warming (Coumou & Rahmstorf, 2012; Rummukainen, 2012; IPCC, 2021). Furthermore, end-users of the SCFs who lack formal meteorological expertise may struggle to accurately interpret the forecasts (Ebhuoma, 2022). As a result, there is a need to provide SCFs that have a broader range of characteristics for the upcoming season. Moreover, it is crucial to enhance their ability to properly interpret and effectively utilize the probabilistic SCFs (Hansen et al., 2022).

Stewart (1988) discovered a substantial correlation between the onset date of rainfall and the length of the seasonal rainfall in 18 African, Asian, Near Eastern, and North American nations. Early-onset seasons were related to longer seasonal rainfall durations and greater amounts of rainfall in this study as compared to late-onset seasons. A similar pattern was discovered in a study conducted in Machakos, Kenya, which discovered a positive relationship between onset dates and seasonal rainfall amount and duration, daily rainfall intensity, and maize productivity (Stewart, 1988). Recent studies in Eastern (MacLeod, 2018; Wakjira et al., 2021) and Western Africa (Obarein & Amanambu, 2019) have discovered that seasonal rainfall onset dates influence cropping decisions, such as crop cultivar selection, as well as seasonal rainfall characteristics, such as seasonal rainfall amounts and frequency and length of the rainy season. This suggests that the growing period conditions and productivity can be predicted by the correlation that exists between the onset dates and rainfall characteristics which largely determine crop performance in rainfed systems. Thus, SCFs that contain rainfall onset date prediction as well as expected average rainfall conditions would benefit smallholder farmers in planning their agricultural activities and managing their crops throughout the season (Mitsui & Boers, 2021). However, detailed studies are needed to determine whether rainfall onset dates can indeed be a good predictor of the characteristics of variables that have a significant impact on crop growth and productivity. Such variables include the frequency and magnitude of dry and wet spells, and the probabilities of exceeding crop water requirements at various scales, such as daily, monthly, and seasonal, and their drivers (Bombardi et al., 2020; She & Xia, 2012).

Degefu et al. (2017) and Hoell and Funk (2014) discovered that the sea surface temperature (SST) over the Indian and Pacific Oceans had a substantial impact on the seasonal rainfall distribution in the Eastern Africa region. Recent studies have also confirmed that remote teleconnections over the Indian (Indian Ocean dipole) and Pacific Oceans (El Nino-Southern Oscillation) have a significant impact on interannual rainfall variability and the frequency of extreme events such as drought and flooding (Palmer et al., 2023; Park et al., 2020). These findings confirmed the assumption that SST over these regions is very likely an important potential driver of rainfall variability in East Africa. Consequently, the opportunity should be taken to further explore the impact of SST on specific rainfall characteristics such as onset and cessation, duration, and amount, etc., in the region. Seasonal rainfall prediction models are designed based on simple to complex statistical methods, including canonical correlation analysis, principal component analysis, and other supervised machine learning algorithms e.g., linear regression, decision trees, random forest, k-Nearest Neighbor, etc. An important criterion of a good rainfall predictor that can be used with these methods is that the predictor's impact on the atmosphere must persist throughout the season—a criterion that is sufficiently met by the SSTs due to their slow evolution (Parker and Diop-Kane, 2017).

1.2. Objectives

The current study aims to assess the benefit of seasonal climate forecasts in predicting growing season conditions and performance, as well as in climate risk management, with a focus on the Kongwa district in central Tanzania. In contrast to the conventional

approach, the study established the use of rainfall onset dates as the criterion for predicting and describing growing period conditions in Kongwa and similar semi-arid environments. The study explored the large-scale atmospheric drivers that influence rainfall onset date patterns and changes in the study region and used the same to predict the onset dates. The latter employs surface temperature (SST) data from the Indian (IOD i.e., Indian Ocean Dipole) and Pacific (NINO3, NINO4, and NINO3.4) ocean regions, as well as a machine-learning algorithm known as a k-nearest neighbor, to forecast seasonal rainfall onset and hence growth period conditions and performance in the study area. To this end, the model's forecast skills are then evaluated using a simple bio-economic model to assess the economic benefits of using SCF in climate risk management.

2. Materials and methods

2.1. Study location and datasets

The present study was conducted in the Kongwa district (center coordinates 6° 12′00″ S, 36° 25′ 00″ E) a semi-arid area located within the Dodoma region at an elevation of approximately 1000 m above sea level. The onset of the monsoon happens around December each year and the monsoon season continues until April to early May the following year. On average, the Kongwa district receives about 520 mm annually, the wettest months being December and January. The climatological mean minimum and maximum daily temperatures are 17 °C and 29 °C, respectively. The soil in the Kongwa district is a freely drained soil characterized by a rise in clay content from 20 % at the surface to at least 30 % at about 50 cm depth. The top layer is acidic (pH less than 5.5) and characterized by low (less than 1.5 %) soil organic carbon contents.

We acquired long-term daily weather records for three stations in the Dodoma region, i.e., Kongwa (1981–2020), Dodoma (1935–2016), and Hombolo (1981–2020) from the Tanzania Meteorological Authority (TMA). These datasets were used in the study to establish a relationship between the growing period rainfall characteristics and the onset date in the region. Crop growth simulation, prediction of the onset dates using the SST, and SCF evaluation were done using the Kongwa district dataset due to the availability of other data such as soil data required for crop modeling. Therefore, a long-term series (1935–2020) of daily rainfall datasets was created. The missing rainfall and temperature data for the Kongwa station from 1935 to 1980 were replaced by the nearby station i.e., Dodoma station – which is located 86 km southwest of the Kongwa station. The two stations share the same climate zone and topography (flat to gently undulating terrain), as well as rainfall and temperature patterns. Moreover, we examined how the Dodoma station data explained the variability and patterns of the Kongwa station seasonal rainfall for the period in which both the dataset had data (1981 – 2015) using the Kling-Gupta Efficiency (KGE) (Knoben et al., 2019) and found the Dodoma dataset reproduced well the rainfall variability and pattern of the Kongwa station (KGE = 0.64). Solar radiation data required for crop model simulation were computed using the Donatelli-Campbell model (Donatelli et al., 1998) which takes daily maximum and minimum temperatures, daily rainfall records, and the latitude of the location as input. Seasonal climate forecasts issued by TMA were obtained from the World AgroMeteorological Information Service website (WAMIS. (n.d.).). The Sea Surface Temperature data required for onset prediction in the machine learning model for the entire period of study were obtained from the Australian Bureau of Meteorology website (http://www.bom.gov.au).

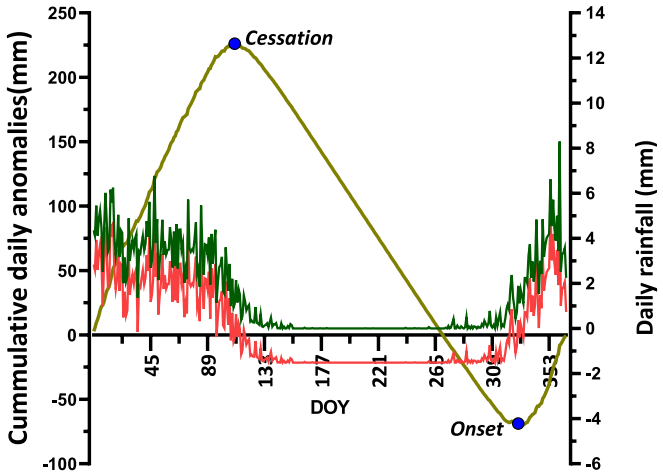

Fig. 1. Liebmann's method for seasonal rainfall onset dates computation is required to predict and characterize the growing period in the Kongwa district. The climatological daily rainfall amounts were averaged over the 1981 to 2020 period. The green and red curves represent the climatological daily mean rainfall and climatological daily mean rainfall anomaly respectively. (For interpretation of the references to colour in this figure legend, the reader is referred to the web version of this article.)

2.2. Seasonal rainfall onset in the study area

For crop production, the onset date should be the one that guarantees the continuity of wet days and provides the initial and likely continued availability of sufficient soil moisture to meet the crop water requirements (Ferijal et al., 2022) for the effective growth and productivity of crops. To satisfy these criteria, the present study used Liebmann's method (Dunning et al., 2016) to determine the seasonal rainfall onset dates due to its suitability for agricultural activities (such as planning of growing period) as reported by Bombardi et al. (2020), Ferijal et al. (2022), Joseph et al (2023), MacLeod (2018), and Wakjira et al. (2021). An advantage of Liebmann's method is that it computes the effective start of the climatological wet period to define the onset date, thus ensuring the wet period's continuation after onset. It consists of the following steps:

From a given daily rainfall data the start of the rainy season is determined first by computing the cumulative daily rainfall anomaly on a day *d, C(d)*, using equation (1) below.

$$\boldsymbol{C(d)} = \sum_{i=1Jan}^{d} \boldsymbol{Q_i} - \overline{\boldsymbol{Q}} \tag{1}$$

whereby i runs from the 1st of January to the 31st of December, $\boldsymbol{Q_i}$ is the climatological mean rainfall for each day of the year, and $\overline{\boldsymbol{Q}}$ is the climatological daily mean rainfall. From equation (1) a curve is plotted (Fig. 1) and the start (d_s) and the end (d_e) of the climatological wet season are determined by the minimum and the maximum in the *C(d)* curve (Fig. 1) respectively. The dates for each year are calculated by computing the daily cumulative rainfall anomaly on days *D, A(D)*, using equation (2).

$$\boldsymbol{A(D)} = \sum_{j=d_s-50}^{D} \boldsymbol{R_j} - \overline{\boldsymbol{Q}} \tag{2}$$

whereby R_j is the rainfall on day j. *A(D)* is calculated for each day from $d_s - 50$ to $d_e + 50$ for each year.

2.3. Post-onset seasonal rainfall characteristics

Crop growth and productivity are significantly impacted by post-onset rainfall characteristics such as rainfall amount and distribution, and the intensity and frequency of wet and dry spells (Bedane et al., 2022). These characteristics largely guide farm-level decisions and impact crop production from local to regional scales. For instance, the intensity and duration of mid-season dry spells significantly impact various farm operations such as weeding, fertilizer, and pesticide applications. Hence, it is important to comprehensively analyze such characteristics to support farm-level decision-making and generate information to support policy-making at different levels or advisory tasks of governmental institutions (e.g., extension services). We used several statistics as described below to analyze various post-onset seasonal rainfall characteristics and characterize the growing period in the study area.

2.3.1. Rainfall amount and distribution

We used the average, coefficient of variation, percentiles, and probability of exceedance to analyze the study area's post-onset rainfall distribution and variability. The average seasonal rainfall and the number of rainy days from 1935 to 2020 were computed between the onset and cessation events. A rainy day refers to a day that receives at least 1 mm of rain (Pohl et al., 2017). The coefficient of variation (CV) was used to measure variability at different temporal scales i.e., seasonal, and monthly, in both rainfall amount and the number of rainy days. The probability of exceedance chart was used to estimate and compare the probabilities of the total rainfall in the early-, normal-, and late-onset seasons required to meet crop minimum water needs e.g., in studies on semi-arid tropical regions have found 450 mm as a threshold for medium (90 to 110 days) to long (at least 110 days) duration maize cultivars (Mebrahtu et al., 2021; Moeletsi & Walker, 2012). The seasons, i.e., early-, normal-, and late-onset, were defined based on the climatological mean and standard deviation of the computed rainfall onset dates. The threshold for the normal-onset season was the one whose onset date was within the lower (climatological mean onset date minus the standard deviation) and upper (climatological mean onset date plus the standard deviation) thresholds, while early- and late-onset seasons were those whose onset dates were below and above the lower threshold and upper threshold, respectively. We used maize as a reference crop to realize the 450 mm threshold because maize is a high-water demand and a very important cereal crop grown in the study area (Garello et al., 2023).

2.3.2. Dry spells frequency and distribution

Several consecutive dry days are referred as to a dry spell (She & Xia,2012). A dry day is a day that receives less than 1 mm of rain (World Meteorological Organization, 2017). The present study examined the frequency and distribution of dry spells 30 days after onset (early dry spells) and within a 50-day window 45 days after onset (mid-season dry spells), to assess the impact of dry spells during the critical crop growth stages. We quantified the mean and maximum dry spell length in the periods among the early-, normal-, and late-onset seasons.

2.4. Crop productivity in relation to post-onset rainfall characteristics

The present study used a process-based, dynamic crop growth model i.e., APSIM (Agricultural Production Systems Simulator) to assess the impacts of post-season rainfall characteristics on the yield of two cereal crops, maize, and sorghum. Over decades, the model

has been tested and proven its robustness and reliability in simulating crop growth and productivity and related processes in subhumid semi-arid environments of Africa (e.g., Akinseye et al. 2017; Hoffmann et al. 2020; Msongaleli et al., 2017; Sultan, 2014; Whitbread et al., 2010) under various farming systems and practices such as conservation agriculture, micro-dosing, intercropping, etc., (Chaki et al., 2022; Holzworth et al., 2014; Nelson et al., 2021). The model simulates the interaction of genotype by environment and management (G x E x M) on a daily time step (Mandrini et al., 2022) to determine crop development (phenology), dry matter accumulation, water use, nitrogen uptake, above-ground and below-ground biomass, grain yield and other output variables. Boote et al. (2021) and Keating et al. (2003) provide more details of the model structure and functionalities including different crops, soil, and management modules as well as various soil processes e.g., water balance, soil organic matter dynamics, mineralization routines, etc.

2.4.1. Calibration and validation of the APSIM model

Normally crop models are calibrated and validated before being used in different environments to ensure their robustness and reliability. However, the APSIM model was originally developed and then widely tested for its robustness and reliability in simulating accurately complex agricultural systems in tropical and semi-arid environments (e.g., Akinseye et al. 2017; Hoffmann et al. 2020; Kisaka et al. 2015; Msongaleli et al., 2017; Rötter & Van Keulen, 1997; Sultan, 2014; Whitbread et al., 2010) similar to that of the current study area. Due to the lack of sufficient high-quality experimental data from the study region, further model evaluation (calibration and validation) was not performed, but we relied on previous successful calibrations and validations which proved the applicability and robustness of the model for applications aligned to the current study's objectives. Model parameterization relied on information from previous studies (see, Keating et al., 2003; Whitbread et al., 2010). For setting up the model, we utilized the parameter values calibrated and validated for the study region by Mbungu et al. (2014) and Msongaleli et al. (2015). These parameters were then used to perform the long-term simulation runs.. The above-mentioned model evaluation studies have reported good agreement between the simulated and observed maize and sorghum yields. For instance, Msongaleli et al. (2015), conducted a study in the Dodoma and Singida regions in Tanzania and reported that about 75 % and 84 % of the maize and sorghum yield variability, respectively, could be explained by the APSIM model.

2.4.2. Set-up of APSIM simulation runs

We then set up long-term maize and sorghum growth simulations to simulate maize and sorghum yield for the entire study period i.e., 1935 to 2020. Both crops were sown within three different windows i.e., 1st to 30th November; 1st to 31st December; and 1st to 31st January, at a plant density of 5 plants m^{-2} upon receiving at least 20 mm of rain in 3 days for maize and 15 plants m^{-2} and row spacing of 600 mm for sorghum. In the sorghum simulation, the cumulative amount of rainfall at sowing was set to zero to include dry sowing events in the simulation. A total of 60 kg ha^{-1} of nitrogen (N) fertilizer was applied 50 % at sowing and 50 % 30 days after sowing. This amount was set to mimic the recommended (Senkoro et al., 2017) amount is 40—–90 kg ha^{-1} in the low-input system like the study areaThe initial soil parameters that were used in the model (Table A.1 in the Appendix) were based on the soil site characterization which was done in 2014 before the start of the experiment. The model reset soil nitrogen and water each year on the 30th of September to avoid the carry-over effect. We reset the initial conditions to isolate the impact of forecasted climatic conditions from inter-annual soil carry-over effects, ensuring that differences in crop performance are directly attributed to the forecasted onset dates and seasonal climatic variability.

2.5. Predicting the growing period conditions using the seasonal climate forecasts

The study predicted growing period conditions using onset dates as a major criterion, moving away from conventional probabilistic information, which can be difficult for farmers to interpret. Onset date predictions offer clear, actionable information for efficient planning and management of the growing season. This study evaluated the forecast skills of seasonal climate forecasts issued by the Tanzania Meteorological Authority (TMA) and compared them with predictions generated using a machine learning model based on the k-Nearest Neighbors (k-NN) algorithm.

TMA provides seasonal forecasts for three major rainfall seasons in Tanzania Masika (March–May) and Vuli (October–December), which dominate the Northeast, Lake Victoria, and coastal zones. Msimu (November–April), which dominates central Tanzania, including the Kongwa district. The forecast skill of TMA's onset date predictions was evaluated using the performance metrics described in the model performance section.

2.5.1. The k-NN model for seasonal climate forecasts

The current study used a machine learning algorithm i.e., k-Nearest Neighbors (k-NN), and the Sea Surface Temperature anomalies (SSTa) over the Indian and Pacific Oceans to predict and characterize the growing period based on the onset dates in the study area. SSTa which form the global climate indices i.e., Indian Ocean Dipole (IOD), NINO3, NINO4, and NINO 3.4, were calculated as an average over the months of July to September. The averages obtained were used in the model as predictors to predict the rainfall onset dates in the study area. The dataset of 85 rainfall seasons from 1935 to 2020 was randomly split in a ratio of 72:28 to train and validate the model. K-Nearest Neighbor is a non-parametric supervised machine-learning classification distance-based algorithm. Prediction of a particular data point class is made by taking the nearest k points to the data point and the weighted average of the classes of the nearest points. The distances between the features of the points are computed using various approaches including Euclidean, Manhattan, and Makowski methods (Appiah-Badu et al., 2022; Hussein et al., 2022). K-NN is a versatile machine-learning algorithm that can be used for both classification and prediction. It has proven to perform well even in predicting seasonal rainfall characteristics with

small datasets (Biruntha et al., 2022; Yu & Haskins, 2021), which makes it suitable for use in data-sparse locations like the Kongwa district.

The model performance of the above-selected algorithms i.e., k-NN, depends on the efficient optimization of the hyperparameters of the algorithm. To overcome the problem of overfitting or underfitting the model, we conducted appropriate hyperparameter optimization before selecting the best model based on performance metrics (Agrawal, 2020; Schratz et al., 2019). The grid search method was used to obtain the most optimized set of hyperparameters for the models. Grid search builds and evaluates the model for each combination of algorithm parameters specified in a grid to achieve the best-optimized hyperparameters (Ranjan et al., 2019). Although this method is time-consuming and computationally expensive, it is still regarded as one of the most accurate methods to tune the hyperparameters (Agrawal, 2020; Ranjan et al., 2019).

It is worth noting that, based on evidence from previous studies (Degefu et al., 2017; Hoell and Funk, 2014), which demonstrated a strong correlation between sea surface temperature anomalies (SSTa) in the Indian and Pacific Oceans and rainfall variability in East Africa, the SSTa were utilized as predictors in our model. However, the current study did not explore the intricate dynamics of these teleconnections, as the focus was on using SSTa as a reliable predictor for rainfall variability.

2.6. Seasonal climate forecasts performance evaluation

The TMA forecasts and the k-NN model's performance were evaluated and compared using various metrics including accuracy, precision, recall, and F1 score (details on these metrics are available in the Appendix). Our interest was to measure how good the forecasts were at predicting growing period conditions and determine the level at which the prediction would be reliable for on-farm decision-making. Thus, the forecast accuracies produced were further evaluated in a bioeconomic model described below.

The bio-economic model used in the present study assumes a linear relationship between the forecast skills and the expected profit—computed by using a profit function. Like previous studies we also assume a farmer is risk-neutral i.e., he/she decides that results in the highest expected profit (An-Vo et al., 2021). To account for variability in yield, product price, and costs of production we included a non-standard Gaussian noise in the profit function equation as shown below:

$$\Pi(\boldsymbol{x_i}) = \boldsymbol{R}(\boldsymbol{x_i}) - \boldsymbol{C}(\boldsymbol{x_i}) + \boldsymbol{\varepsilon} \tag{3}$$

where $\Pi(\boldsymbol{x_i})$ is the net profit, $\boldsymbol{R}(\boldsymbol{x_i})$ total revenues generated, $\boldsymbol{C}(\boldsymbol{x_i})$ is the cost of production, and $\boldsymbol{\varepsilon}$ is the non-standard Gaussian noise which accounts for variability in the cost of production and revenue generated by achieving yield $\boldsymbol{x}$ in a particular year $\boldsymbol{i}$. The expected profit based on the forecast $\boldsymbol{f}$ of probability $\boldsymbol{p}$ was then computed using the following equation:

$$\mathbf{E}[\boldsymbol{profit}|\boldsymbol{f} = \boldsymbol{p}] = (\boldsymbol{f} = \boldsymbol{p}) \times \boldsymbol{P}_{50^{th}} \{\boldsymbol{V}_{\Pi(\boldsymbol{x})}\} \tag{4}$$

whereby $\boldsymbol{f}$ is the season rainfall onset forecast i.e., early-, normal-, and late-onset seasons. $\boldsymbol{p}$ is the likelihood of the forecast having values ranging from 0 to 1 whereby a value closer to 1 represents a more accurate forecast. $\boldsymbol{V}_{\Pi(\boldsymbol{x})}$ is a set of the profit generated in the entire period of study. We took the $\boldsymbol{P}_{50^{th}}$(50th percentile) value of the generated profits as the most robust value of the profit generated that is unaffected by extreme values or outliers in the distribution. Economic data on maize and sorghum i.e., cost of production, selling price, and minimum profit required to sustain the production system, were primarily obtained from the focus group discussions conducted with 60 lead farmers from six villages in Kongwa (in 2021/22) and complemented by secondary data published on the Ministry of Agriculture website and previous studies in the region (Kalema et al., 2022; Ministry of Agriculture, 2023; Utonga, 2022). The cost of producing maize and sorghum per ton was $230, and $155 respectively while the average selling price per ton of grain maize and sorghum in the 2021/22 season were $361 and $500 respectively. Moreover, the farmers mentioned that the minimum profit required to sustain the production system in maize and sorghum were $650 and $400 respectively. The USD to TZS exchange rate used in the present study was 1 USD = TZS 1800—an average of minimum and maximum exchange rates within the past 20 years obtained from https://www.exchangerates.org/. The results obtained were used to establish a threshold of reliability of the seasonal forecast and compare the two sources of forecast used in the present study to meet farmers' requirements for effective climate risk management.

3. Results

3.1. Seasonal rainfall onset in the study area

The onset dates were computed, and the average was calculated among various climatological periods i.e., 1935 – 1964, 1951 – 1980, 1981–2010, and 1991 – 2020 to examine if there exist significant changes in onset dates among the climatological periods. We found the average onset dates and their corresponding standard deviation of these same climatological periods were 9th December ± 15 days, 6th December ± 12 days, 8th December ± 15 days, and 8th December ± 15 days respectively. Our analysis showed the four climatological periods considered the rainfall started around the 6th to 9th of December and thus confirmed insignificant changes in the time series. The average onset date and its corresponding standard deviation over the study period were found to be 7th December ± 14 days. Thus, the so-called mean or normal-onset dates ranged from 24th November to 21st December. The onset dates before 24th November were regarded as early-onset dates while those after 21st December were regarded as late-onset dates. The post-onset seasonal rainfall characteristics analyzed in the following section were based on these three groups. We investigated the occurrence of false onset in the early-, normal-, and late-seasons. The term "false onset" refers to a rainy event(s) that occurs between October 1

and the minimum onset date of the onset season, which includes early-, normal-, and late-onset seasons. We found that late-onset seasons had a higher frequency (33 %) of at least three rainfall incidents before the effective onset than early- and normal-onset seasons, which had 7 % and 18 %, respectively.

3.2. Post-onset seasonal rainfall characteristics

3.2.1. Seasonal rainfall amount and distribution

We computed the post-onset seasonal rainfall amount and duration to characterize the rainfall behavior in the study area for the entire period of the study i.e., 1935—2020. Our analyses showed that the seasonal rainfall amount and distribution among the three groups i.e., early-, normal, and late-onset seasons differed greatly (Fig. 2a). The average seasonal rainfall amounts in the early-, normal-, and late-onset seasons were 650 mm, 508 mm, and 425 mm respectively. The late-onset seasons showed the highest within-season rainfall variability (CV = 28 %) compared to early- and normal-onset seasons whose CVs were 23 % and 27 %, respectively. The average number of rainy days was higher in the early-onset seasons (48 rainy days) compared to both normal- (35 days) and late-onset (32 days) seasons (Fig. 2b). Moreover, the highest variability in rainy days per season was shown in the late-onset seasons (CV = 25 %) and the lowest was in the normal and early-onset seasons which both had a CV of 21 %. The statistical test we conducted revealed significant differences (p-values < 0.0003) between the seasonal rainfall amounts and rainy days among the three groups (Tables B.1 and B.2 in the Appendix). Tukey's post hoc test revealed significant differences between early- and late-onset, and early and normal onset seasons (Tables B.3 and B.4 in the Appendix). The average amount of rainfall and rainy days in the normal- and late-onset groups insignificantly differed (p-values > 0.05).

Fig. 2 below shows the probabilities of exceedance in both seasonal rainfall amount and duration. The early-onset seasons showed the highest probability (93 %) of exceeding the threshold value i.e., 450 mm, compared to normal and late-onset seasons whose probabilities to exceed 450 mm per season were less than 60 % (Fig. 2a). This implies that the early-onset seasons exceeded 450 mm in 9 out of 10 while the normal and late-onset seasons exceeded 450 mm only in about 5 out of 10 seasons. In Fig. 2b, the early-onset seasons showed the highest probability (85 %) of getting at least 35 days—80 % of the average annual rainy days—compared to normal- and late-onset seasons which had a probability of less than 50 % of getting at least 35 rainy days. Similar results were obtained at nearby meteorological stations, namely Hombolo and Dodoma (see Fig. B.1 in the Appendix). In at least 9 out of 10 seasons, the early-onset season exceeded 450 mm and had a greater than 50 % chance of exceeding the average number of rainy days per season. The normal- and late-onset seasons, on the other hand, had a lower probability (< 80 %) of exceeding 450 mm and the average number of rainy days in both Hombolo and Dodoma.

3.2.2. Monthly rainfall distribution

On average, between November and April, the early-, normal, and late-onset seasons received 112 mm, 89 mm, and 77 mm monthly respectively. The variability was very high in the normal and late-onset seasons—49 % and 62 % respectively—compared to early-onset seasons (CV = 33 %). The wettest months in the early-onset seasons were December and January in which the rainfall amounts received were at least 138 mm per month while in the normal and late-onset seasons, the wettest month was January which received at least 120 mm per month. The monthly variation in both rainfall amounts, and duration is very high (CV > 30) in the early-, normal, and late-onset seasons. However, the variability is much higher in November and December for normal and late-onset seasons as compared to early-onset seasons (Table 1).

3.2.3. Daily rainfall intensity and distribution

We examined the daily rainfall intensity distribution in the study area among the three season categories i.e., early-, normal-, and

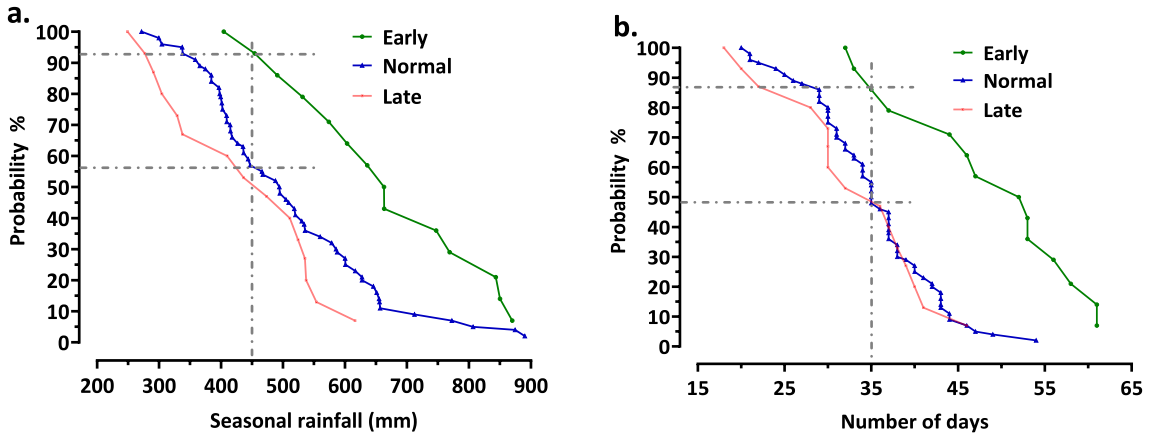

Fig. 2. Probability of exceedance charts showing the distribution of seasonal (a) rainfall amount and (b) rainy days in early-, normal-, and late-onset seasons in Kongwa from 1935 to 2020.

late-onset seasons. The daily rainfall averages were computed for each day of the year during the wet period i.e., November to April. Our analyses show the rainfall events in the early-onset seasons were characterized by the highest rainfall amounts compared to normal- and late-onset seasons (Fig. 3). For the normal- and late-onset seasons, approximately half of the daily rainfall amounts ranged between 1 and 5 mm. Notably, the normal-onset seasons had the highest percentage (71 %) of rainfall events within this range. Rainfall events with daily amounts greater than 5 mm were more common in the early-onset seasons when compared to other seasons. In the early-, normal-, and late-onset seasons, respectively, 21 %, 10 %, and 15 % of the daily rainfall amounts were greater than 5 mm.

3.2.4. Dry spells frequency and distribution

Fig. 4 shows the post-onset distribution of dry spells among the seasons. The 80th percentile of dry spell events of a particular season was computed to characterize dry spell events distribution in 4 out of 5 seasons. Our analysis showed that the distribution of dry spell events among the early-, normal-, and late-onset seasons was statistically insignificant in both 30 days after onset and mid-season periods (Tables B.5 and B.6 **in the** Appendix). However, in the mid-season, the dry spell events of 4 to 8 days were slightly higher in normal- and late-onset seasons as compared to early-onset seasons.

Fig. 5 highlights the frequency distribution of the maximum dry spells of length "*n*"—whereby *n* is an integer: *n = 1, 2, 3…,30*—in the study area 30 days after onset and in a 50-day window 45 days after onset (mid-season). Maximum dry spells of 4 to 14 days a month after onset were possible in both early-, normal-, and late-onset seasons, however, their frequencies were between 10 and 35 %. The maximum dry spells of more than 14 days were also possible in normal- and late-onset seasons. Similarly, in about 3 out of 10 seasons, the maximum dry spells of at least 10 days were observed in the early- and late-onset seasons during the mid-season periods. The maximum dry spells of more than 10 days were also observed in both seasons however their frequencies were less than 20 %.

The overall distribution of maximum dry spells in the first month after the onset date and in the mid-season slightly differed among the rainfall seasons i.e., early-, normal-, and late-onset seasons. On average, the early-onset seasons had a maximum dry spell of 9 and 13 days during the first month after onset and in the mid-season respectively. The normal-onset seasons had maximum dry spells of 10 and 15 days after the onset date and in the mid-season respectively. However, the late-onset seasons had the maximum dry spell of 11 days in both the 30 days after onset and the mid-season periods.

3.3. Crop productivity in relation to post-onset rainfall characteristics

We analyzed simulated maize and sorghum yield distributions in the early-, normal-, and late-onset seasons among the three sowing windows (Fig. 6). In the early-onset seasons, the average maize yield in the November sowing window was slightly higher contrary to the normal- and late-onset seasons whose average yields in the November sowing window were lower compared to December and January sowing windows. Moreover, the maize yield variabilities in the November sowing windows were higher in both early-onset (CV = 23 %), normal-onset (CV = 43 %), and late-onset (CV = 68 %) seasons compared to December and January sowing windows whose CV values ranged from 10 % to 22 %. In contrast, the sorghum average yields were highest ($\geq$1.5 t ha^{-1}) in the November sowing window in late-onset seasons and lowest ($\leq$ 0.9 t ha^{-1}) in the same sowing window in the early-onset seasons (Fig. 6**b**). Other sowing windows had sorghum average yields between 1.0 to 1.3 t ha^{-1}. Like maize yields, the sorghum variabilities were higher in the November sowing window in both early-onset (CV = 44 %), normal-onset (CV = 43 %), and late-onset (CV = 39 %) seasons compared to December and January sowing windows whose CV values ranged from 11 % to 30 %.

Statistical tests were performed to examine the significance of the differences that existed in the simulated maize and sorghum yields in different rainfall onset dates and sowing windows. The simulated yields' variances for both crops were unequal across the onset and sowing dates and thus a Weighted Least Squares analysis in a linear model was used to investigate the effect of rainfall onset dates—early-, normal-, and late-onset—and sowing windows—November, December, and January—in simulated maize yields. Our analyses revealed significant differences in maize yield simulated within different rainfall onset dates (value $<$ 0.0001), sowing windows (p-value $\leq$ 0.001), and their interaction (p-value $\leq$ 0.004) (**in the** Appendix). Fig. 7**a** shows the November sowing window had higher yields—above the overall average yield (2.48 t ha^{-1})—in early-onset seasons and very poor yields in normal- and late-onset seasons. Moreover, the December and January sowing windows had good yields (at least 2.48 t ha^{-1}) in the early- and normal-onset seasons. The late-onset seasons had lower yields i.e., below the overall average (2.48 t ha^{-1}), in all three sowing windows.

Onset dates contributed insignificantly to the sorghum simulated yield variation (p-value $>$ 0.1), whereas the sowing windows contributed significantly to simulated yield variations (p-value $<$ 0.000). However, the interaction effect of onset dates and sowing

Table 1
Monthly rainfall (measured in mm) and the number of rainy days distribution in the early-, normal-, and late-onset seasons. In the parenthesis is their corresponding coefficient of variation in %. *RD = Rainy days*.

Month	Early-onset		Normal-onset		Late-onset	
	Rainfall	RD	Rainfall	RD	Rainfall	RD
Nov	92(55)	6(50)	14(136)	1(100)	9(167)	1(100)
Dec	169(36)	11(36)	121(52)	8(38)	39(113)	3(67)
Jan	138(49)	11(45)	126(63)	8(50)	129(45)	8(50)
Feb	101(76)	8(50)	106(59)	8(50)	108(63)	8(50)
Mar	108(61)	9(56)	108(53)	8(38)	113(58)	9(44)
Apr	63(79)	6(50)	59(95)	5(60)	61(66)	7(57)

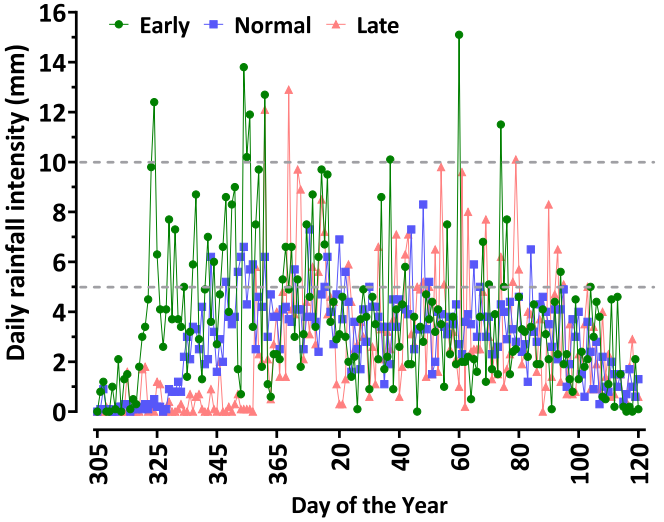

Fig. 3. Distribution of average daily rainfall intensity in the study area among the three season categories i.e., early-, normal-, and late-onset seasons.

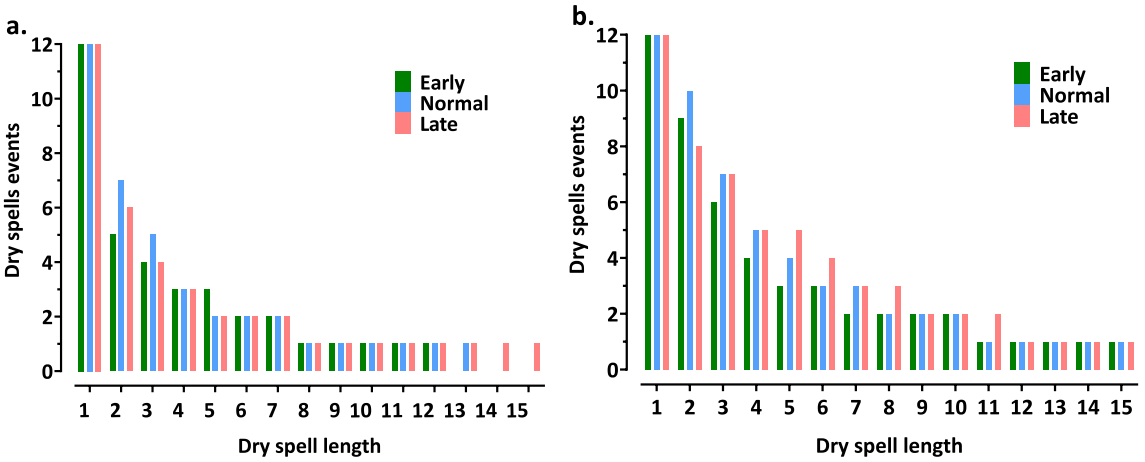

Fig. 4. Dry spell events distribution at the 80th percentile in the study area(a) 30 days after onset date, (b) within a 50-day window 45 days after onset i.e., mid-season dry spells in the early-, normal-, and late-onset seasons.

window significantly accounts for the simulated yield variations (p-value < 0.05). Fig. 7**b** shows the late-onset seasons had slightly higher sorghum simulated yields i.e., above the overall average (1.16 t ha^{-1}), compared to early- and normal-onset seasons.

3.4. Seasonal climate forecasts performance evaluation

We compared the performance in predicting the seasonal rainfall onset dates using the four-performance metrics i.e., accuracy, precision, recall, and F1-score. Our analyses showed that in about 8 out of 10 seasons, the k-NN model predicted correctly (accuracy = 79 %) the onset dates in the study region while the TMA forecast had about 5 out of 10 seasons predicted correctly (accuracy = 79 %) (Table 2). Moreover, the k-NN model predictions had higher scores (≥70 %) in all other metrics i.e., precision, recall, and F1-score compared to the TMA predictions which had scores between 46 – 62 % of the performance metrics used.

Fig. 8**a** shows a maize farmer can achieve at least $650 per ton (the minimum amount of the profit required to sustain production) in the early-onset season if the forecast accuracy is at least 60 % while the same amount can be achieved in the early, normal- and late-onset season if the forecast accuracy is at least 70 %, 90 %, and 97 % respectively. The forecast accuracies below the aforementioned thresholds were more likely to lead to a loss of farmers' investment. In sorghum (Fig. 8**c**), the highest profits were observed in the late-onset seasons and the lowest profits were observed in the early-onset seasons. To achieve at least $400 per ton given that a farmer fully integrates the seasonal forecast, the forecast accuracy should be at least 83 %. Our analyses showed making decisions e.g., sowing, for both crops without prior knowledge of the coming season i.e., sowing in November, December, and January, had a low probability

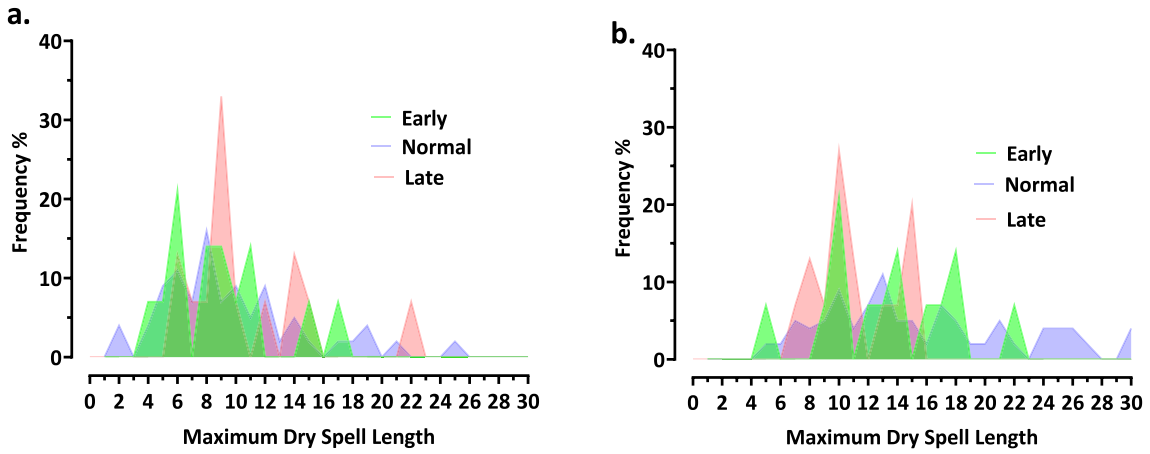

Fig. 5. Frequency of occurrence of post-onset maximum dry spells length(a) 30 days after onset data, (b) within a 50-day window 45 days after onset i.e., mid-season dry spells.

(≤70 %) of getting at least $650 and $400 for maize and sorghum respectively and was associated with a higher chance (≥80 %) of getting very low profit (<$200) or losses especially in the November sowing window (Fig. 9**b and d**).

4. Discussion

4.1. Post-onset rainfall characteristics in the study area

The SST over the Indian and Pacific Ocean regions was found to be an important driver of rainfall variability in the study (Palmer et al., 2023; Park et al., 2020) and a significant predictor of rainfall onset dates in the present study. The onset dates were discovered to better depict the growing period characteristics, including the variability and distribution of rainfall throughout the season. We found 7th December as the average rainfall onset date and the early- and late-onset seasons were between late November and December respectively. The computed onset dates implied the beginning of the growing period—the period in which the farmers sow and harvest their crops— was between November and December and they were consistent with the cropping calendar of the study area as described in previous studies (e.g., FEWS NET, 2017).

Our analyses, like previous studies, confirmed a strong relationship between seasonal rainfall onset dates and both the amount and duration of seasonal rainfall (MacLeod, 2018; Obarein & Amanambu, 2019) and portrayed the late-onset seasons were riskier for crop production compared to normal- and early-onset seasons. At both the seasonal and monthly scales, early-onset seasons were associated with the highest average amounts of rainfall and number of rainy days compared to both normal- and late-onset seasons. The early-onset seasons were much wetter and longer allowing farmers to have more crop options and wider sowing windows than in the normal- and late-onset seasons (Guido et al., 2020). The late-onset seasons had the greatest variability in both amount and duration of rainfall which made them riskier for the growth and productivity of high-water demand crops such as maize, but they could be beneficial for low-water demand crops such as sorghum (Bedane et al., 2022; Pokhrel et al., 2019).

Our analyses showed the beginning of the growing period had a higher chance of having critical water stress conditions due to high variability in rainfall distribution in the normal- and late-onset seasons compared to early-onset seasons. The months of November and December in normal- and late-onset seasons were characterized by the highest variability and lowest amount of rainfall. Moreover, the lower probability of getting an amount greater than 450 mm per season in the late-onset season, presented in the probability of exceedance charts in the results section, confirmed the unreliability of the late-onset seasons in the production of high-water demand crops such as maize (Moeletsi & Walker, 2012). These results suggest climate risk management in the study area requires efficient pre-season crop planning based on the anticipated type of the season e.g., crop diversification, to increase the resiliency, productivity, and sustainability of the current production system.

Like previous studies (Barron et al., 2003; Marteau et al., 2011), our analyses showed that the frequency and length of dry spells also depend on rainfall onset dates and thus characterize the corresponding growing period. We found dry spells of 8 to 10 days one month after onset were more frequent in the normal and late-onset seasons compared to the early-onset season. Moreover, the mid-season dry spells of at least 14 days were possible in the late-onset season—although less frequent—indicating a higher possibility of water stress in the late-onset seasons which may lead to a substantial crop yield reduction (Bal et al., 2022; Barron et al., 2003). In addition to dry spell distribution, daily rainfall intensity was an important indicator of the differences between the seasons. We found the daily rainfall intensity and distribution differed between the early-, normal-, and late-onset seasons. In contrast to the normal- and late-onset seasons, rainfall events of at least 5 mm per day were more frequent in the early-onset seasons, i.e., late November to mid-January, indicating differences at the beginning of the wet period that supports various agricultural operations.

In both the 30 days after onset and the mid-season periods, our analyses revealed a statistically insignificant difference in dry spell length and frequency between the early-, normal-, and late-onset seasons. The intensity of daily rainfall following the dry spells, on the

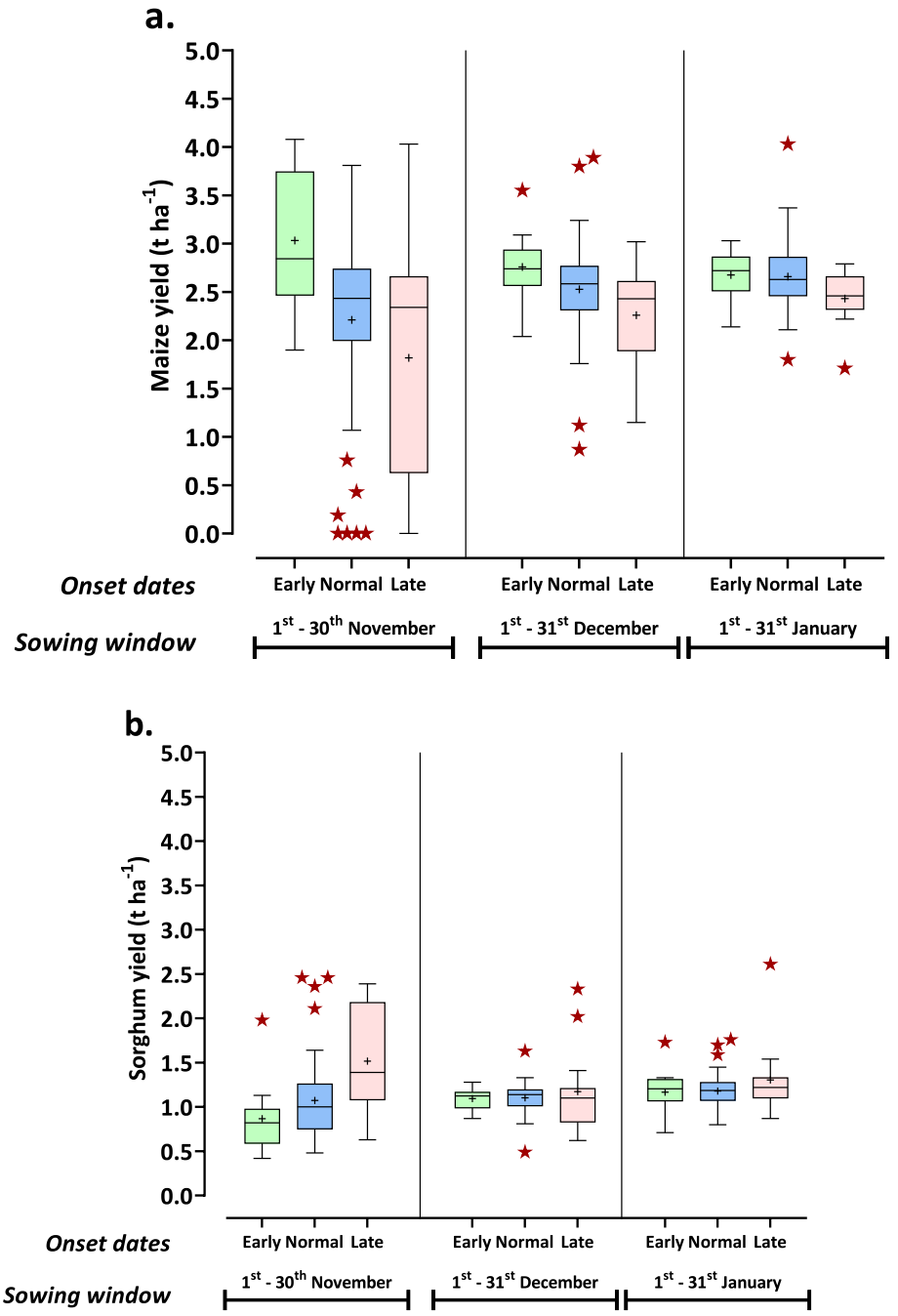

Fig. 6. Simulated yield distributions for (a) maize and (b) sorghum in the early-, normal-, and late-onset seasons among the three sowing windows, i.e., November, December, and January.

other hand, created a significant difference between seasons in terms of total rainfall at different scales, i.e., weekly, monthly, and seasonally, as well as water availability during the growing season. Moisture stresses caused by dry spells can be mitigated to some extent in good soil with high water holding capacity in the early-onset seasons, as opposed to the normal- and late-onset seasons. Our findings suggest that the planning and timing of on-farm operations such as sowing, thinning, and fertilizer application should be prioritized differently in the early-, normal- and late-onset seasons to fully take advantage of each season's potential, effectively manage climate risks, and increase productivity (Guido et al., 2020).

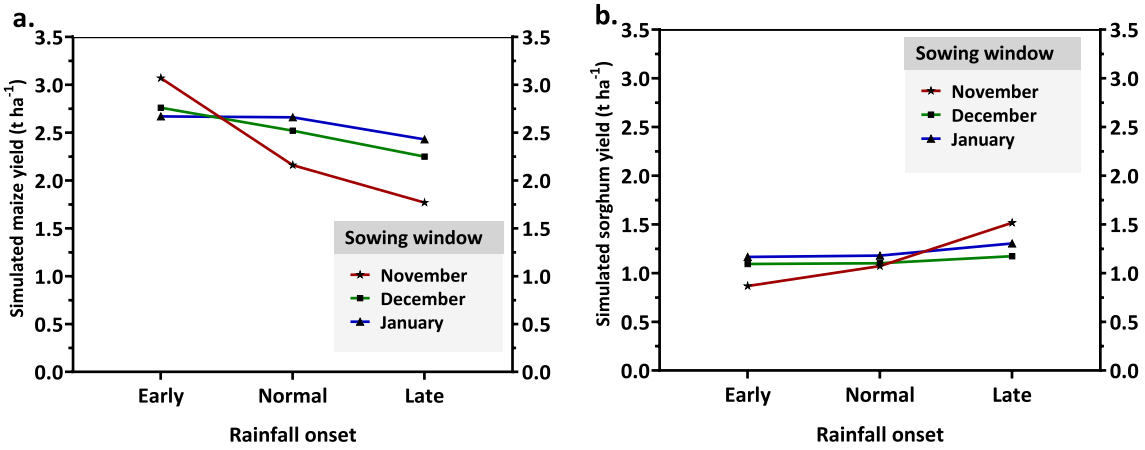

Fig. 7. Main effects plots of the yield distributions of (a) maize and (b) sorghum under different sowing windows over early-, normal-, and late-onset seasons.

Table 2
Comparison of the performance—computed as the weighted average of a particular metric—of the TMA and k-NN seasonal rainfall onset prediction in the study area.

Forecast	Performance metric (%)			
	Accuracy	Precision	Recall	F1-score
k-NN	79	84	79	74
TMA	46	62	46	46

4.2. Simulated maize and sorghum yield distribution in the study area

The characteristics of the growing period as predicted by the onset dates strongly influenced the maize and sorghum productivity in the study area. The highest maize yields were obtained in the early-onset seasons compared to the normal- and late-onset seasons. The early-onset seasons were characterized by higher amounts and longer duration of seasonal rainfall compared to the normal and late-onset seasons, which ensured the availability of sufficient soil moisture for growth and productivity. Similarly, Omoyo et al. (2015) and Rowhani et al. (2011) found a positive relationship between maize yields and seasonal rainfall, i.e., higher maize yields during higher rainfall seasons and vice versa. This means that obtaining an in-depth understanding of the relationship between rainfall variability and crop output in the study area is a key first step toward developing adaptation strategies and effectively reducing the consequences of climate change and variability.

We found maize yield variabilities in the study area were also explained by sowing dates. Sowing in November showed the highest variation in the simulated maize yields compared to December and January sowing windows in all the seasons. Furthermore, as in previous studies, we found that simulated maize yields were affected by both the type of growing season and the timing of sowing. (Maresma et al., 2019). Therefore, to increase crop production in the study area, management practices such as timely sowing, weeding, fertilizer, and pesticide application should be thoroughly considered (Xiong & Tarnavsky, 2020).

Variations in the sorghum simulated yield were determined by both rainfall seasonal types—early-, normal-, and late-onset seasons—and sowing windows—November, December, and January. Compared to other sowing windows and rainfall season types, the November sowing window had the highest sorghum yield in the late-onset seasons and the lowest sorghum yield in the early-onset seasons. Our results imply that the sorghum cultivar used in the present study (*Macia*) produced more yields when sown during the dry period followed by the rainfall period. Jabereldar et al. (2017) attributed the higher sorghum yield obtained when the crop is sown in a dry period followed by wet spells with higher water use efficiency, which resulted in better growth and productivity of sorghum. However, the amount of sorghum yield produced in the study area (Msongaleli et al., 2017) usually does not reach the potential yield due to various factors including poor management practices, climate risks such as drought, and poor soil fertility (Mwamahonje et al., 2021). This necessitates the need to revise the current policies to support agricultural management practices, climate change adaptation strategies, and improve soil fertility to increase sorghum yield in the study area.

The assessment of crop yield distribution in various season types conducted in the present study suggests in the season where moisture conditions are predicted to be insufficient, sorghum can be a good alternative to minimize losses and improve food security. However, climate information systems, external and internal markets, and agricultural input supplier systems should be strengthened to reduce the risk of losing farmers' investments.

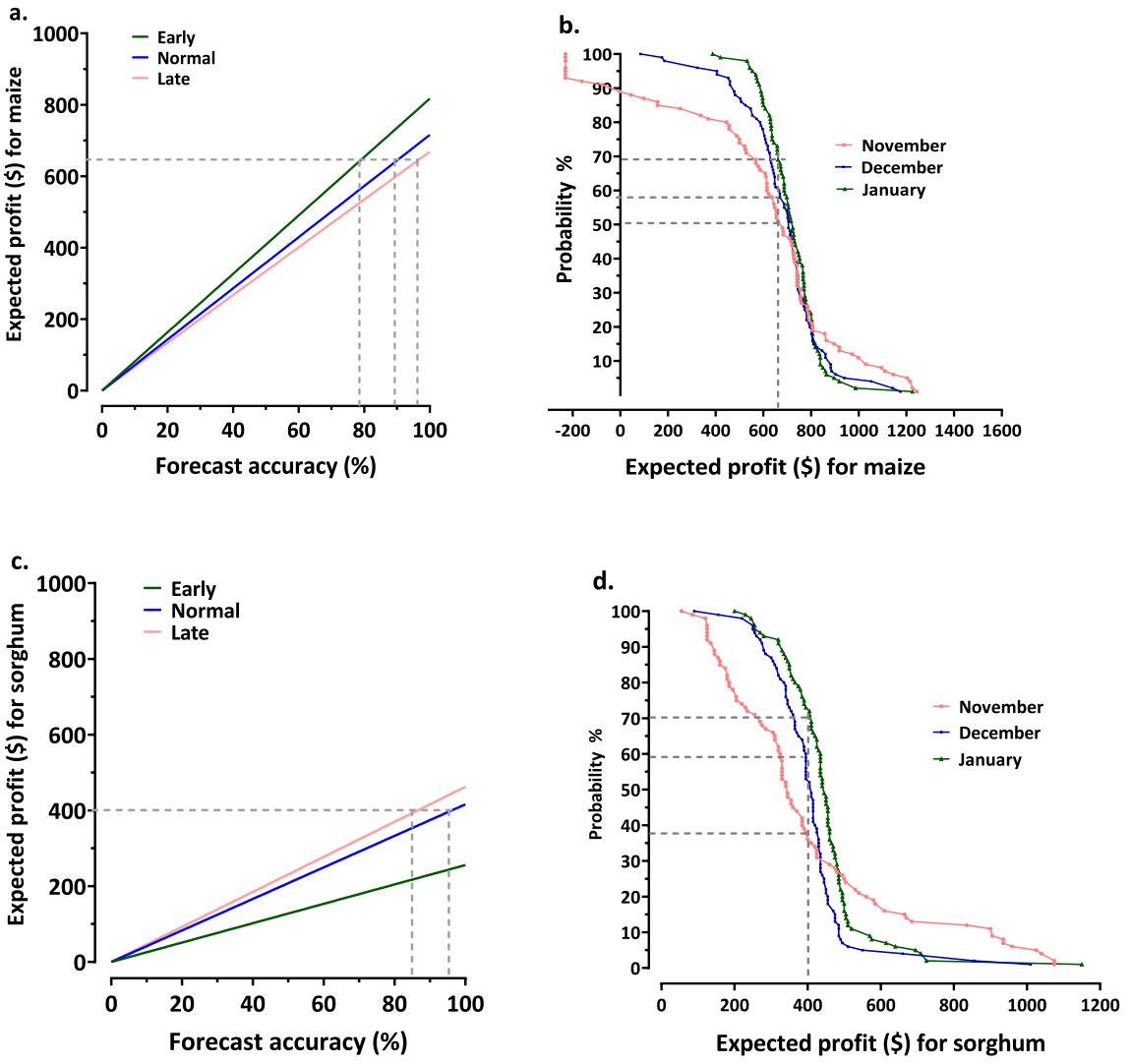

Fig. 8. An estimate of the expected profit for maize (a) and sorghum(c) when a farmer made crucial decisions, such as sowing decisions, totally based on the forecast provided. When an early-onset season is forecast, for example, a farmer will plant his or her crops in the early sowing window and not otherwise. The probabilities of getting the minimum profit required to sustain the production of maize and sorghum without integration of seasonal forecast are presented in (b) and (d) respectively.

4.3. Seasonal climate forecasts performance evaluation

Like previous studies (Degefu et al., 2017) we found the SSTa were a good predictor of rainfall onset dates which served as a reliable criterion for the prediction of other rainfall characteristics such as amount and distribution. In rain-fed systems, these characteristics are crucial components of climate risk management in crop production. Therefore, the SSTa evolution before and during the season can provide valuable insight to enhance climate risk management in the study area. We found the k-NN predictive model, created in the present study which used the SSTa over the Indian and Pacific oceans, had the best performance in predicting and characterizing the growing period using the onset dates in the study area compared to TMA seasonal climate forecasts. This implies that machine learning algorithms such as k-NN can be reliably used to produce seasonal rainfall predictions (Mitsui & Boers, 2021; Shah et al., 2018), but their usefulness may be limited by data scarcity. Furthermore, our analyses revealed that the k-NN model had the best F1-score when compared to the TMA forecast, indicating its superior ability to predict the early-, normal-, and late-onset seasons in the study area, which is an important component when farmers integrate seasonal forecasts in climate risk management.

Our findings indicate that using skilled seasonal climate forecasts (Rauch et al., 2019) which best inform the seasonal rainfall characteristics for climate risk management can be economically profitable (An-Vo et al., 2021) for both maize and sorghum production, provided the forecasts are timely and understandable to end users (Ebhuoma, 2022). Our analyses suggest that seasonal climate forecasts when used to predict the growing period conditions, i.e., provide information on rainfall amounts, onset dates, dry

spell frequency, and so on, would be beneficial to smallholder farmers in terms of facilitating timely farm operations, better managing of climate risks, and returning farmers' investments. We also found that ignoring seasonal climate forecasts was riskier, particularly in late-onset seasons. For example, in late-onset seasons, sowing decisions made without prior awareness of the upcoming seasonal characteristics were more likely to result in losses in maize and sorghum production. In contrast, the incorporation of seasonal forecasts with at least 80 % accuracy for both maize and sorghum production helped farmers improve tactical management, thereby increasing productivity and decreasing yield losses.

4.4. Limitations

It is vital to note that the current study has certain limitations. First, due to a lack of on-farm agronomic data, this study's evaluation of the potential use of seasonal forecasts to predict the growing season conditions and its associated risks in maize and sorghum production is limited to a few interventions, such as the use of improved varieties and appropriate sowing dates. However, if good-quality data are available, the current study might be expanded to include more climate-smart interventions, such as conservation agriculture, crop diversification, agroforestry, and so on, and investigate how these practices might be influenced by seasonal climate forecasts. Second, the current study assessed system performance using seasonal climate forecasts, the accuracy of which is low due to the influence of different atmospheric variables and their interactions, which are difficult to anticipate over extended periods. However, most agricultural activities that influence system performance occur within the first 30 to 45 days of the growing season. As a result, the low-accuracy seasonal climate forecast can be complemented by sub-seasonal forecasts to better manage climate risks and boost system productivity, which was not examined in the current study. Third, k-NN was the only machine-learning algorithm employed in the current study; however, other machine-learning algorithms may produce better results. As a result, a comparison study of different machine-learning algorithms for predicting seasonal rainfall characteristics is required.

5. Conclusion

The application of SCF in climate risk assessment and management for crop production in semi-arid environments is highly recommended. However, for SCF to be reliably integrated into farmers' decision-making, they must demonstrate high accuracy. For example, our study showed that a forecast skill of at least 79 % is required for farmers to effectively utilize the information, reduce risks, and achieve a return on their investment. For our study area in Kongwa, Tanzania, we demonstrated significant benefits in reducing the impact of climate change and variability on crop production. We found SSTs to be good predictors of seasonal rainfall onset, which can be reliably utilized to predict the growing period conditions and manage climate risks in crop production. We have shown the use of SCF to predict the growing season conditions and manage climate risks based on the rainfall onset date criterion – which turned out to be beneficial both agronomically and economically. Agronomically, it boosted system production, and economically, it reduced the financial risk related to farmers' investments. However, for smallholder farmers to fully exploit these benefits, an improved network of extension agents is necessary for farmers to access and use SCF to improve agricultural practices and effectively manage and reduce climate risks. As a result, the government must invest in strengthening the infrastructure needed for the development and dissemination of meteorological information including the SCF.

CRediT authorship contribution statement

Jacob Emanuel Joseph: Writing – review & editing, Writing – original draft, Visualization, Methodology, Formal analysis, Data curation, Conceptualization. **K.P.C Rao:** Writing – review & editing, Validation, Resources, Methodology, Formal analysis, Conceptualization. **Elirehema Swai:** Writing – review & editing, Validation, Resources, Data curation. **Anthony M. Whitbread:** Writing – review & editing, Validation, Supervision, Methodology, Funding acquisition, Conceptualization. **Reimund P. Rötter:** Writing – review & editing, Validation, Supervision, Resources, Methodology, Conceptualization.

Declaration of competing interest

The authors declare that they have no known competing financial interests or personal relationships that could have appeared to influence the work reported in this paper.

Acknowledgments

This research was funded by the Academy for International Agricultural Research (ACINAR), commissioned by the German Federal Ministry for Economic Cooperation and Development (BMZ), and implemented by ATSAF e.V. on behalf of the Deutsche Gesellschaft für Internationale Zusammenarbeit (GIZ) GmbH. We also gratefully acknowledge the support of the Tropical Plant Production and Agricultural Systems Modelling (TROPAGS) division in the Department of Crop Sciences at the University of Göttingen, Germany. Additionally, we extend our appreciation to the International Livestock Research Institute (ILRI) for funding the contributions of Jacob Emanuel Joseph and Anthony M. Whitbread to this study.

Appendix

A: Description of characteristics in the study location

Soil properties.

Table A1
Soil properties of the study area and initial values used in APSIM simulation by layer. All values were measured at the experimental site in 2014, except for those marked with an asterisk (*). These were estimated using appropriate methods or obtained from published sources.

Layer number	1	2	3	4	5
Layer depth (mm)	100	100	200	420	380
Airdry weight (mm/mm) *	0.060	0.090	0.150	0.180	0.200
LL15(mm/mm)	0.150	0.150	0.150	0.180	0.200
DUL (mm/mm)	0.273	0.273	0.301	0.351	0.351
SAT (mm/mm)*	0.404	0.404	0.461	0.451	0.457
SWCON*	0.7	0.7	0.7	0.7	0.7
Bulk density (g cm^{-3})	1.30	1.17	1.14	1.20	1.30
Organic carbon (%)	0.585	0.585	0.410	0.293	0.273
pH	5.84	5.84	5.13	5.51	5.61
NH_4	0.200	0.150	0.100	0.025	0.025
NO_3	0.667	0.500	0.333	0.333	0.167
Finert*	0.40	0.50	0.80	0.95	0.95
Fbiom*	0.035	0.02	0.015	0.015	0.01

B: Seasonal rainfall characteristics in the Kongwa district

Statistical analyses of the differences between the onset groups.

Analysis of variance (ANOVA) summary Table for the average amount of rainfall in (B.1) and number of rainy days (B.2) among the three groups of seasons i.e., normal-, normal-, and late-onset seasons.

Table B1

Source of variation	DF	Sum Sq	Mean Sq	F value	P(>F)
Between Onset dates definitions	2	377298	188649	9.764	0.0002
Residuals	82	1584257	19320		

Table B2

Source of variation	DF	Sum Sq	Mean Sq	F value	P(>F)
Between Onset dates definitions	2	2113	1056	16.60	0.0001
Residuals	82	5219	63.65		

Tukey multiple comparisons of the average amount of rainfall in (B.3) and number of rainy days (B.4) among the three groups of seasons i.e., normal-, normal-, and late-onset seasons.

Table B3

Test	Mean Diff.	95.% CI of diff.	Adjusted P Value
Early vs. Late	224.3	101.0 to 347.6	0.0001
Early vs. Normal	142.2	43.01 to 241.3	0.0028
Late vs. Normal	−82.13	−178.6 to 14.34	0.1109

Table B4

Test	Mean Diff.	95.% CI of diff.	Adjusted P Value
Early vs. Late	15.25	8.171 to 22.32	<0.0001
Early vs. Normal	12.63	6.935 to 18.32	<0.0001
Late vs. Normal	−2.623	−8.159 to 2.914	0.4981

Analysis of variance (ANOVA) summary Table for dry spell events distribution at the 80th percentile in the study area (B.5) 30 days after onset data, (B.6) within a 50-day window 45 days after onset i.e., mid-season dry spells in the early-, normal-, and late-onset seasons.

Table B5

Source of variation	DF	Sum Sq	Mean Sq	F value	P(>F)
Between Onset dates definitions	2	0.044	0.022	0.002	0.998
Residuals	42	502	11.96		

Table B6

Source of variation	DF	Sum Sq	Mean Sq	F value	P(>F)
Between Onset dates definitions	2	1.378	0.689	0.03	0.966
Residuals	42	833	19.85		

Seasonal rainfall characteristics in relation to onset in the Dodoma region

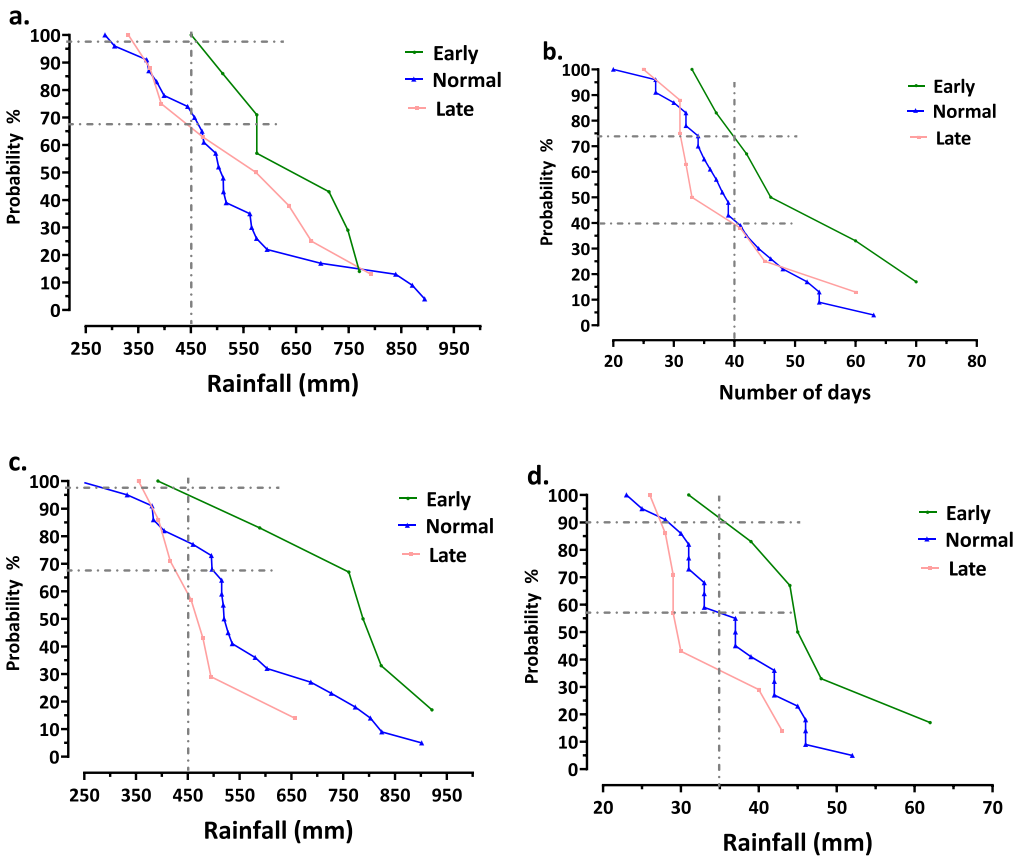

Fig. B1. Probability of exceedance charts showing the distribution of seasonal rainfall amount in Hombolo (a) and Dodoma (c) and the rainy days in Hombolo (b) and Dodoma (d) in early-, normal-, and late-onset seasons.

C: Yield Distribution in different onset dates.

Analysis of variance (ANOVA) summary Table for the impact of different rainfall onset dates and sowing windows on simulated (C.1) maize and (C.2) sorghum yields in the study area.

Table C1

Source	DF	Seq SS	Seq MS	F-Value	P-Value
Onset	2	15.870	7.9348	25.10	0.000
Sowing	2	13.097	6.5483	20.71	0.000
Onset*Sowing	4	4.965	1.2413	3.93	0.004
Error	246	77.777	0.3162		
Total	254	111.708			

Table C2

Source	DF	Seq SS	Seq MS	F-Value	P-Value
Onset	2	0.7345	0.3673	1.85	0.160
Sowing	2	14.9741	7.4870	37.65	0.000
Onset*Sowing	4	1.9702	0.4926	2.48	0.045
Error	246	48.9164	0.1988		
Total	254	66.5952			

D: Performance metrics

Table D1

Definition and formula of performance metrics used in the present study.

Metric	Definition	Purpose	Formula
Accuracy	Measures the overall proportion of correct predictions (both positives and negatives).	Evaluates the general performance of the model across all classes.	$\text{Accuracy} = \frac{TP + TN}{TP + TN + FP + FN}$
Precision (P)	Measures how many of the predicted positive instances are actually correct.	Focuses on minimizing false positives.	$P = \frac{TP}{TP + FP}$

(*continued on next page*)

Table D1 (*continued*)

Metric	Definition	Purpose	Formula
Recall (R)	Measures the proportion of actual positive instances correctly identified.	Highlights the model's ability to detect all relevant cases, critical for minimizing false negatives (e.g., rainfall events detection).	$R = \frac{TP}{TP + FN}$
F1 Score	The harmonic mean of Precision and Recall, balancing the two metrics.	Provides a single performance score, especially useful for imbalanced datasets.	$F1 = 2 \cdot \frac{P \cdot R}{P + R}$

Data availability

The authors do not have permission to share data.

References

Agrawal T. (2020). Hyperparameter Optimization in Machine Learning: Make Your Machine Learning and Deep Learning Models More Efficient. Apress.

Akinseye, F.M., Adam, M., Agele, S.O., Hoffmann, M.P., Traoré, P.C.S., Whitbread, A.M., 2017. Assessing crop model improvements through comparison of sorghum (sorghum bicolor L. moench) simulation models: a case study of West African varieties. Field Crop Res 201, 19–31. https://doi.org/10.1016/j.fcr.2016.10.015.

An-Vo, D., Radanielson, A.M., Mushtaq, S., Reardon-Smith, K., Hewitt, C., 2021. A framework for assessing the value of seasonal climate forecasting in key agricultural decisions. Clim. Serv. 22, 100234. https://doi.org/10.1016/j.cliser.2021.100234.

Appiah-Badu, N.K.A., Missah, Y.M., Amekudzi, L.K., Ussiph, N., Frimpong, T., Ahene, E., 2022. Rainfall prediction using machine learning algorithms for the various ecological zones of Ghana. IEEE Access 10, 5069–5082. https://doi.org/10.1109/access.2021.3139312.

Araya, A., Keesstra, S., Stroosnijder, L., 2010. A new agro-climatic classification for crop suitability zoning in northern semi-arid Ethiopia. Agric. For. Meteorol. 150 (7–8), 1057–1064. https://doi.org/10.1016/j.agrformet.2010.04.003.

Bal, S.K., Sandeep, V., Kumar, P.V., Rao, A.S., Pramod, V., Manikandan, N., Rao, C.S., Singh, N.P., Bhaskar, S., 2022. Assessing impact of dry spells on the principal rainfed crops in major dryland regions of India. Agric. For. Meteorol. 313, 108768. https://doi.org/10.1016/j.agrformet.2021.108768.

Barron, J., Rockström, J., Gichuki, F., Hatibu, N., 2003. Dry spell analysis and maize yields for two semi-arid locations in east Africa. Agric. For. Meteorol. 117 (1–2), 23–37. https://doi.org/10.1016/s0168-1923(03)00037-6.

Bedane, H.R., Beketie, K.T., Fantahun, E.E., Feyisa, G.L., Anose, F.A., 2022. The impact of rainfall variability and crop production on vertisols in the central highlands of Ethiopia. Environ. Syst. Res. 11 (1). https://doi.org/10.1186/s40068-022-00275-3.

Biruntha, S., Sowmiya, B.S., Subashri, R., Vasanth, M., 2022. Rainfall prediction using kNN and decision tree. In: 2022 International Conference on Electronics and Renewable Systems (ICEARS). https://doi.org/10.1109/icears53579.2022.9752220.

Bombardi, R.J., Moron, V., Goodnight, J.S., 2020. Detection, variability, and predictability of monsoon onset and withdrawal dates: a review. Int. J. Climatol. 40 (2), 641–667. https://doi.org/10.1002/joc.6264.

Boote, K.J., Adam, M., Ahmad, I., Ahmad, S., Cammarano, D., Chattha, A.A., Claessens, L., Dimes, J., Durand, W., Freduah, B.S., Gummadi, S., Hargreaves, J.N.G., Hoogenboom, G., Tui, S.H., Jones, J.W., Khaliq, T., MacCarthy, D.S., Masikati, P., McDermid, S.P., Wajid, S.A., 2021. Understanding differences in climate sensitivity simulations of APSIM and DSSAT crop models. In: In WORLD SCIENTIFIC (EUROPE). https://doi.org/10.1142/9781786348791_0002.

Ceglar, A., Toreti, A., 2021. Seasonal climate forecast can inform the European agricultural sector well in advance of harvesting. npj Clim. Atmos. Sci. 4 (1). https://doi.org/10.1038/s41612-021-00198-3.

Chaki, A.K., Gaydon, D.S., Dalal, R.C., Bellotti, W.D., Gathala, M.K., Hossain, A., Menzies, N.W., 2022. How we used APSIM to simulate conservation agriculture practices in the rice-wheat system of the Eastern Gangetic Plains. Field Crop Res 275, 108344. https://doi.org/10.1016/j.fcr.2021.108344.

Coumou, D., Rahmstorf, S., 2012. A decade of weather extremes. Nat. Clim. Chang. 2 (7), 491–496. https://doi.org/10.1038/nclimate1452.

Degefu, M.A., Rowell, D.P., Bewket, W., 2017. Teleconnections between Ethiopian rainfall variability and global SSTs: observations and methods for model evaluation. Meteorol. Atmos. Phys. 129 (2), 173–186. https://doi.org/10.1007/s00703-016-0466-9.

Diouf, N.S., Ouedraogo, M., Ouedraogo, I., Ablouka, G., Zougmoré, R., 2020. Using seasonal forecast as an adaptation strategy: gender differential impact on yield and income in senegal. Atmos. 11 (10), 1127. https://doi.org/10.3390/atmos11101127.

Dunning, C.M., Black, E., Allan, R.P., 2016. The onset and cessation of seasonal rainfall over Africa. J. Geophys. Res. Atmos. 121 (19). https://doi.org/10.1002/2016jd025428.

Ebhuoma, E.E., 2022. Factors undermining the use of seasonal climate forecasts among farmers in south africa and zimbabwe: implications for the 1st and 2nd sustainable development goals. Front. Sustainable Food Syst. 6. https://doi.org/10.3389/fsufs.2022.761195.

Ferijal, T., Batelaan, O., Shanafield, M., Alfahmi, F., 2022. Determination of rainy season onset and cessation based on a flexible driest period. Theor. Appl. Climatol. 148 (1–2), 91–104. https://doi.org/10.1007/s00704-021-03917-1.

FEWS NET. (2017, October). Famine Early Warning Systems Network-Tanzania. Retrieved February 28, 2023, from https://fews.net/east-africa/tanzania.

Garello, F.J., Ploschuk, E.L., Melani, E.M., Taboada, M.A., 2023. Soil water availability and water absorption by maize in sodic soils with high water table. Field Crop Res 295, 108877. https://doi.org/10.1016/j.fcr.2023.108877.

Guido, Z., Zimmer, A., Lopus, S., Hannah, C., Gower, D., Waldman, K., Krell, N., Sheffield, J., Caylor, K., Evans, T., 2020. Farmer forecasts: impacts of seasonal rainfall expectations on agricultural decision-making in Sub-Saharan Africa. Clim. Risk Manag. 30, 100247. https://doi.org/10.1016/j.crm.2020.100247.

Hansen, J., Dinku, T., Robertson, A.W., Cousin, R., Trzaska, S., Mason, S.J., 2022. Flexible forecast presentation overcomes longstanding obstacles to using probabilistic seasonal forecasts. Front. Clim. 4. https://doi.org/10.3389/fclim.2022.908661.

Hoell, A., Funk, C., 2014. Indo-Pacific sea surface temperature influences on failed consecutive rainy seasons over eastern Africa. Clim. Dyn. 43 (5–6), 1645–1660. https://doi.org/10.1007/s00382-013-1991-6.

Hoffmann, M.P., Swanepoel, C.M., Nelson, W., Beukes, D.J., Van Der Laan, M., Hargreaves, J.N.G., Rötter, R.P., 2020. Simulating medium-term effects of cropping system diversification on soil fertility and crop productivity in southern Africa. Eur. J. Agron. 119, 126089. https://doi.org/10.1016/j.eja.2020.126089.

Holzworth, D.P., Huth, N.I., deVoil, P.G., Zurcher, E.J., Herrmann, N.I., McLean, G., Chenu, K., Van Oosterom, E.J., Snow, V., Murphy, C., Moore, A.D., Brown, H., Whish, J.P., Verrall, S., Fainges, J., Bell, L.W., Peake, A.S., Poulton, P.L., Hochman, Z., Keating, B.A., 2014. APSIM – evolution towards a new generation of agricultural systems simulation. Environ. Modelling & Software 62, 327–350. https://doi.org/10.1016/j.envsoft.2014.07.009.

Hussein, E.A., Ghaziasgar, M., Thron, C., Vaccari, M., Jafta, Y., 2022. Rainfall prediction using machine learning models: literature survey. Artificial Intelligence for Data Science in Theory and Practice 75–108. https://doi.org/10.1007/978-3-030-92245-0_4.

Inthavong, T., Tsubo, M., Fukai, S., 2011. A water balance model for characterization of length of growing period and water stress development for rainfed lowland rice. Field Crop Res 121 (2), 291–301. https://doi.org/10.1016/j.fcr.2010.12.019.

IPCC. (2021). Summary for Policymakers. In V. Masson-Delmotte, P. Zhai, A. Pirani, S. L. Connors, C. Péan, S. Berger, et al., (Eds.), *Climate Change 2021:* The Physical Science Basis. Contribution of Working Group I to the Sixth Assessment Report of the Intergovernmental Panel on Climate Change (pp. 3–32). Cambridge University Press. Doi: 10.1017/9781009157896.001.

Jabereldar, A.A., Naim, A.M.E., Abdalla, A.R., Dagash, Y.M.I., 2017. Effect of water stress on yield and water use efficiency of sorghum (sorghum bicolor L. Moench) in semi-arid environment. international. J. Agric. For. 7 (1), 1–6. http://www.sapub.org/global/showpaperpdf.aspx?doi=10.5923/j.ijaf.20170701.01.

Jätzold, R., Kutsch, H., 1982. Agro-Ecological Zones of the Tropics, with a Sample from Kenya. Der Tropenlandwirt – J. Agric. Tropics and Subtropics 83 (1), 15–34. https://www.jarts.info/index.php/tropenlandwirt/article/download/1533/707.
Joseph, J.E., Akinseye, F.M., Worou, O.N., Faye, A., Konte, O., Whitbread, A.M., Rötter, R.P., 2023. Assessment of the relations between crop yield variability and the onset and intensity of the West African Monsoon. Agric. For. Meteorol. 333, 109431. https://doi.org/10.1016/j.agrformet.2023.109431.
Kalema, E.P., Akpo, E., Muricho, G., Ringo, J.H., Ojiewo, C.O., Varshney, R.K., 2022. Mapping out market drivers of improved variety seed use: the case of sorghum in Tanzania. Heliyon 8 (1), e08715. https://doi.org/10.1016/j.heliyon.2022.e08715.
Keating, B., Carberry, P.S., Hammer, G., Probert, M.E., Robertson, M.J., Holzworth, D., Huth, N.I., Hargreaves, J.N.G., Meinke, H., Hochman, Z., McLean, G., Verburg, K., Snow, V., Dimes, J., Silburn, M., Wang, E., Brown, S., Bristow, K., Asseng, S., Smith, C.J., 2003. An overview of APSIM, a model designed for farming systems simulation. Eur. J. Agron. 18 (3–4), 267–288. https://doi.org/10.1016/s1161-0301(02)00108-9.
Knoben, W., Freer, J., Woods, R., 2019. Technical note: inherent benchmark or not? Comparing Nash–Sutcliffe and Kling–Gupta efficiency scores. Hydrol. Earth Syst. Sci. 23 (10), 4323–4331. https://doi.org/10.5194/hess-23-4323-2019.
MacLeod, D., 2018. Seasonal predictability of onset and cessation of the east African rains. Weather Clim. Extremes 21, 27–35. https://doi.org/10.1016/j.wace.2018.05.003.
Mandrini, G., Archontoulis, S.V., Pittelkow, C.M., Mieno, T., Martin, N.F., 2022. Simulated dataset of corn response to nitrogen over thousands of fields and multiple years in Illinois. Data Brief 40, 107753. https://doi.org/10.1016/j.dib.2021.107753.
Maresma, A., Ballesta, A., Santiveri, F., Lloveras, J., 2019. Sowing date affects maize development and yield in irrigated mediterranean environments. Agriculture 9 (3), 67. https://doi.org/10.3390/agriculture9030067.
Marteau, R., Sultan, B., Moron, V., Alhassane, A., Baron, C., Traoré, S.B., 2011. The onset of the rainy season and farmers' sowing strategy for pearl millet cultivation in Southwest Niger. Agric. For. Meteorol. 151 (10), 1356–1369.
Mbungu W., Mahoo H. F., Tumbo S. D., Kahimba F., Rwehumbiza F. B., Mbilinyi B. (2014). Using Climate and Crop Simulation Models for Assessing Climate Change Impacts on Agronomic Practices and Productivity. In Springer eBooks (pp. 201–219). Doi: 10.1007/978-3-319-09360-4_10.
Mebrahtu, Y., Mehari, H., Nurga, Y., Tamiru, H., 2021. Estimation of crop water requirement using CROPWAT model for Maize, A case study of Raya Azebo District, Ethiopia. J. Resources Development and Management. https://doi.org/10.7176/jrdm/74-03.
Ministry of Agriculture. (2023, January 4). Ministry of Agriculture, United Republic of Tanzania. Retrieved March 31, 2023, from https://www.kilimo.go.tz/resources/category/publications.
Mitsui, T., Boers, N., 2021. Seasonal prediction of Indian summer monsoon onset with echo state networks. Environ. Res. Lett. 16 (7), 074024. https://doi.org/10.1088/1748-9326/ac0acb.
Moeletsi, M., Walker, S., 2012. Rainy season characteristics of the Free State Province of South Africa with reference to rain-fed maize production. Water SA 38 (5). https://doi.org/10.4314/wsa.v38i5.17.
Msongaleli, B.M., Rwehumbiza, F.B., Tumbo, S.D., Kihupi, N.I., 2015. Impacts of climate variability and change on rainfed sorghum and maize: implications for food security policy in Tanzania. J. Agric. Sci. 7 (5). https://doi.org/10.5539/jas.v7n5p124.
Msongaleli, B.M., Tumbo, S.D., Kihupi, N.I., Rwehumbiza, F.B., 2017. Performance of sorghum varieties under variable rainfall in central Tanzania. Int. Scholarly Res. Notices 2017, 1–10. https://doi.org/10.1155/2017/2506946.
Mwamahonje, A., Eleblu, J.S.Y., Ofori, K., Deshpande, S., Feyissa, T., Bakuza, W.E., 2021. Sorghum production constraints, trait preferences, and strategies to combat drought in Tanzania. Sustainability 13 (23), 12942. https://doi.org/10.3390/su132312942.
Nelson, W.C.D., Hoffmann, M.P., Vadez, V., Rötter, R.P., Koch, M., Whitbread, A.M., 2021. Can intercropping be an adaptation to drought? A model-based analysis for pearl millet–cowpea. J. Agron. Crop Sci. 208 (6), 910–927. https://doi.org/10.1111/jac.12552.
Obarein, O.A., Amanambu, A.C., 2019. Rainfall timing: variation, characteristics, coherence, and interrelationships in Nigeria. Theor. Appl. Climatol. 137 (3–4), 2607–2621. https://doi.org/10.1007/s00704-018-2731-y.
Omoyo, N.N., Wakhungu, J.W., Oteng'i, S., 2015. Effects of climate variability on maize yield in the arid and semi arid lands of lower eastern Kenya. Agric. & Food Security 4 (1). https://doi.org/10.1186/s40066-015-0028-2.
Palmer, P.I., Wainwright, C.M., Dong, B., Maidment, R.I., Wheeler, K., Gedney, N., Hickman, J.E., Madani, N., Folwell, S.S., Abdo, G., Allan, R.P., Black, E.C.L., Feng, L., Gudoshava, M., Haines, K., Huntingford, C., Kilavi, M., Lunt, M., Shaaban, A.A., Turner, A.G., 2023. Drivers and impacts of Eastern African rainfall variability. Nat. Rev. Earth Environ. https://doi.org/10.1038/s43017-023-00397-x.
Park, S., Kang, D., Yoo, C., Im, J., Lee, M., 2020. Recent ENSO influence on East African drought during rainy seasons through the synergistic use of satellite and reanalysis data. ISPRS J. Photogramm. Remote Sens. 162, 17–26. https://doi.org/10.1016/j.isprsjprs.2020.02.003.
Pohl, B., Macron, C., Monerie, P.A., 2017. Fewer rainy days and more extreme rainfall by the end of the century in Southern Africa. Sci. Rep. 7 (1). https://doi.org/10.1038/srep46466.
Pokhrel, P., Ohgushi, K., Fujita, M., 2019. Impacts of future climate variability on hydrological processes in the upstream catchment of Kase River basin, Japan. Appl. Water Sci. 9 (1). https://doi.org/10.1007/s13201-019-0896-x.
Ranjan, G.S.K., Kumar Verma, A., Radhika, S., 2019. K-nearest neighbors and grid search CV based real time fault monitoring system for industries. In: 2019 IEEE 5th International Conference for Convergence in Technology (I2CT). https://doi.org/10.1109/i2ct45611.2019.9033691.
Rauch, M., Bliefernicht, J., Laux, P., Salack, S., Waongo, M., Kunstmann, H., 2019. Seasonal forecasting of the onset of the rainy season in West Africa. Atmos. 10 (9), 528. https://doi.org/10.3390/atmos10090528.
Rowhani, P., Lobell, D.B., Linderman, M., Ramankutty, N., 2011. Climate variability and crop production in Tanzania. Agric. For. Meteorol. 151 (4), 449–460. https://doi.org/10.1016/j.agrformet.2010.12.002.
Rummukainen, M., 2012. Changes in climate and weather extremes in the 21st century. WIREs Clim. Change 3 (2), 115–129. https://doi.org/10.1002/wcc.160.
Schratz, P., Muenchow, J., Iturritxa, E., Richter, J., Brenning, A., 2019. Hyperparameter tuning and performance assessment of statistical and machine-learning algorithms using spatial data. Ecol. Model. 406, 109–120. https://doi.org/10.1016/j.ecolmodel.2019.06.002.
Shah, U., Garg, S., Sisodiya, N., Dube, N., Sharma, S.A., 2018. Rainfall prediction: accuracy enhancement using machine learning and forecasting techniques. Grid Computing. https://doi.org/10.1109/pdgc.2018.8745763.
Shah, H., Siderius, C., Hellegers, P., 2021. Limitations to adjusting growing periods in different agroecological zones of Pakistan. Agr. Syst. 192, 103184. https://doi.org/10.1016/j.agsy.2021.103184.
She, D., Xia, J., 2012. The spatial and temporal analysis of dry spells in the Yellow River basin, China. Stoch. Env. Res. Risk A. 27 (1), 29–42. https://doi.org/10.1007/s00477-011-0553-x.
Stewart J. I. (1988). Response Farming in Rainfed Agriculture.
Sultan, B., 2014. Robust features of future climate change impacts on sorghum yields in West Africa. Iopscience. https://iopscience.iop.org/article/10.1088/1748-9326/9/10/104006.
Utonga, D., 2022. Analysis of maize profitability among smallholder farmers in Mbinga District, Tanzania. Int. J. Res. Publication and Rev. 1031–1035. https://doi.org/10.55248/gengpi.2022.3.2.13.
Wakjira, M.T., Peleg, N., Anghileri, D., Molnar, D., Alamirew, T., Six, J., Molnar, P., 2021. Rainfall seasonality and timing: implications for cereal crop production in Ethiopia. Agric. For. Meteorol. 310, 108633. https://doi.org/10.1016/j.agrformet.2021.108633.
WAMIS. (n.d.). World AgroMeteorological Information Service. Retrieved March 7, 2023, from http://wamis.org/countries/tanzania.php.
Whitbread, A., Robertson, M., Carberry, P., Dimes, J., 2010. How farming systems simulation can aid the development of more sustainable smallholder farming systems in southern Africa. Eur. J. Agron. 32 (1), 51–58. https://doi.org/10.1016/j.eja.2009.05.004.

World Meteorological Organization. (2017). WMO Guidelines on the Calculation of Climate Normals: Weather Climate Water (2017 edition, Vol. 1203). https://library.wmo.int/doc_num.php?explnum_id=4166.

Xiong, W., Tarnavsky, E., 2020. Better agronomic management increases climate resilience of maize to drought in tanzania. Atmos. 11 (9), 982. https://doi.org/10.3390/atmos11090982.

Yu N., Haskins,T. (2021). KNN, An Underestimated Model for Regional Rainfall Forecasting. arXiv (Cornell University). Doi: 10.48550/arxiv.2103.15235.